J Appl Electrochem (2008) 38:385–394
DOI 10.1007/s10800-007-9451-9

ORIGINAL PAPER

Electroless deposition of ternary Ni–P alloy coatings containing tungsten or nano-scattered alumina composite on steel

Abdel Salam Hamdy · M. A. Shoeib · H. Hady · O. F. Abdel Salam

Received: 9 July 2007 / Revised: 8 November 2007 / Accepted: 8 November 2007 / Published online: 24 November 2007

Abstract The performance of ternary electroless deposited Ni–P–W and Ni–P–alumina composite coatings on low carbon steel substrates was studied. The effect of experimental parameters, such as temperature, pH, nickel sulfate concentration, sodium hypophosphite concentration, sodium citrate concentration, and deposition time on the deposition rate were investigated. The coating brightness, coherence, and uniform surface distribution were improved due to addition of W and alumina. The coating performance was evaluated based on the wear-resistance, micro-hardness, and corrosion resistance. The Ni–P–W ternary alloy coatings showed the highest micro hardness, wear-resistance, brightness, and corrosion resistance. The improvement in the performance of Ni–P–W coatings can be explained by the formation of a tungsten phosphide phase.

Keywords Ternary alloy coatings · Electroless deposition · Ni–P–W · Ni–P–Al_2O_3 composite coatings · Wear · Micro-hardness · Corrosion · EIS

1 Introduction

Nickel–phosphorous (Ni–P) coatings are widely used in many industrial applications due to their outstanding mechanical and chemical properties, such as high hardness and good corrosion/wear-resistance [1–3]. Ni–P coatings can be fabricated by various techniques including electroplating [4] and electroless deposition [5, 6]. Nickel electroplating is used in decorative engineering and electroforming and can also be applied to improve corrosion resistance in industrial equipment. Despite the benefits of a Ni–P coating, the coatings have some weaknesses. First, to achieve a high corrosion resistance, the Ni–P coating must have an electrodeposited chromium layer applied on top, making it a more detailed process. Another substantial drawback is that Ni–P coating processes are incapable of completely coating complicated shapes [7].

Electroless plating is an autocatalytic process, which is widely used for the production of uniform, adherent films for many industrial applications. It can be carried out via the redox reaction of an oxidizer and a reductant in an electrolyte solution [6].

The main reasons for the widespread industrial use of electroless nickel plating are to be found in the unique properties of electroless nickel deposits. An advantage of electroless nickel plating is its ability to coat interior surfaces of pipes, valves, and other parts, on a variety of materials, including metals, plastics, glass, and ceramics [8, 9]. Based on the excellent properties of the coatings, the electroless deposition of Ni–P has been widely investigated [10–13].

Promising results on optimizing the characteristics of the Ni–P system by the introduction of a third element to form ternary Ni–P-based alloy coating have been recently reported. The ternary systems that have been studied include Ni–Cu–P [14, 15], Ni–W–P [16–18], Ni–Re–P, and Ni–Zn–P [19].

Zhao et al. [20] reported that tungsten has an increased importance in ternary alloy coating systems, namely, Ni–

A. S. Hamdy (✉) · M. A. Shoeib
Department of Surface Technology and Corrosion Protection, Central Metallurgical Research and Development Institute, CMRDI, 87, Helwan, Cairo, Egypt
e-mail: ashamdy@cmrdi.sci.eg

H. Hady
Saqr Factory for Advanced Military Industries, Cairo, Egypt

O. F. A. Salam
Faculty of Engineering, University of Cairo, Cairo, Egypt

W–P alloy. It was found that including tungsten in binary Ni–P deposit increases the deposition rate, while improving properties such as hardness, thermal stability, and wear and corrosion resistance [21–23].

A combination of dissimilar materials such as alumina or SiC can produce a composite coating with wide mechanical, chemical, electrical, magnetic, and optical properties. However, these properties depend upon the contribution from the distributed and the matrix phases of the composite material. Metal matrix composites containing ceramic particles as a distributed phase find application in the field of engineering as anti-wear and anti-frictional materials [24].

There are a number of methods of preparation of particle-dispersed metal matrix composites [25]. However, the most common method is composite plating. The incorporation of particles such as alumina into a metal matrix by this method is based on the electro- [1] and electroless [26] plating technique. Recently, a solid powder of primary particles, such as alumina of diameter below 100 nm, was used as the additional ingredient of the nickel composite [27, 28].

Interest is growing in Ni–P coatings for the corrosion protection of steel [13–21]. However, most of the previous studies are focusing on the effect of phosphorous ratio in the binary alloy coating [13, 17, 19–21].

The aim of this work is to study the effect of the experimental parameters on the electroless deposition of high performance Ni–P alloy coatings onto steel substrates using H_2PO_2 as reducing agent from solution containing nickel sulfate, sodium citrate, ammonium sulfate, and other additives such as lactic acid and lead acetate. A series of alloy coatings were prepared at different temperatures and pH. The coatings were evaluated based on their brightness, wear-resistance, micro-hardness, surface distribution, and corrosion resistance. Electrochemical impedance spectroscopy was used to evaluate the coatings performance after 2 weeks of immersion in 3.5% NaCl. The effect of tungsten or alumina particles addition to the Ni–P films on the corrosion resistance, wear-resistance, and micro-hardness was also measured.

2 Experimental

2.1 Materials

Specimens of low carbon steel, in the form 30 × 30 mm taken from sheet of 1-mm thick were used. The nominal composition was as follows (wt.%): 0.025 C; 0.087 Si; 0.44 Mn; 0.002 Cr; 0.0009 Mo; 0.0005 Al; 0.0005 Ni; 0.029 Co; 0.0003 Cu; 0.0006 Nb; 0.013 Ti; 0.026 V; 0.011 W; 0.011 Pb; remainder Fe.

2.2 Coatings

2.2.1 *Surface preparation*

Each specimen was abraded to an 800 grit finish with SiC paper, degreased in acetone, washed with distilled water, and dried in dry air. The specimens were then subjected to ultrasonic cleaning in deionized water. All specimens were etched in a sulfuric acid solution for 3 min and then rinsed with deionized water and acetone and weighed prior to the plating process.

2.2.2 *Bath composition and Ni–P alloy coating preparation*

Nickel–phosphorus (Ni–P) coatings. The binary Ni–P alloy coating was prepared with a composition of 90 wt.% Ni and 10 wt.% P using the electroless plating bath composition given in Table 1.

Nickel-phosphorus-tungsten (Ni–P–W) coatings. The deposition of electroless Ni–W–P alloy was carried out using the bath composition shown in Table 2. The bath pH was adjusted with ammonium hydroxide to 9 ± 0.05. The electroless plating were performed in a glass beaker containing 250 cm^3 of electroless plating solution, which was placed in a large water bath controlled by a contact thermometer. The temperature of the autocatalytic reaction was maintained at 70 ± 1 °C, and the plating time was 1 h. The deposition rate was calculated by weight gain

Table 1 Composition of Ni–P electroless plating bath

Chemicals	Concentration (g L^{-1})
Nickel sulfate, $NiSO_4 \cdot 6$	25
Sodium hypophosphite, $NaH_2PO_2 \cdot H_2O$	25
Sodium citrate, $Na_3C_6H_5O_7 \cdot 2H_2O$	50
Ammonium sulfate, $(NH_4)_2SO_4$	28
Lactic acid, $CH_3CHOHCOOH$	5×10^{-3}
Lead acetate, $Pb(CH_3CO_2)_2 \cdot 3H_2O$	2×10^{-3}

Table 2 Composition of electroless plating bath used for Ni–P–W

Chemicals	Concentration (g L^{-1})
Nickel sulfate, $NiSO_4 \cdot 6H_2O$	25
Sodium tungstate, $Na_2WO_4 \cdot 2H_2O$	5, 25, 45, 65
Sodium hypophosphite, $NaH_2PO_2 \cdot H_2O$	25
Sodium citrate, $Na_3C_6H_5O_7 \cdot 2H_2O$	50
Ammonium sulfate, $(NH_4)_2SO_4$	28
Lactic acid, $CH_3CHOHCOOH$	5×10^{-3}
Lead acetate, $Pb(CH_3CO_2)_2 \cdot 3H_2O$	2×10^{-3}

(mg cm^{-2} h^{-1}). The concentration of sodium tungstate is ranging from 5 to 65 g L^{-1}. The coating composition at different concentrations of sodium tungstate (wt.%) was given in Table 3.

Nickel–phosphorus–aluminum oxide (Ni–P–Al_2O_3) coatings. The deposition of electroless Ni–P–Al_2O_3 composite coating was carried out using the bath composition shown in Table 4.

The bath pH was adjusted with ammonium hydroxide to 9 ± 0.05. The electroless plating were performed in a glass beaker containing 250 cm^3 of electroless plating solution which was placed in a large water bath controlled by contact thermometer. The temperature of the autocatalytic reaction was maintained at 70 ± 1 °C, and the plating time was 1 h. The deposition rate was calculated by weight gain (mg cm^{-2} h^{-1}). The samples were rotated in the bath to ensure uniform contact with homogenized solution. The concentration of Al_2O_3 is ranging from 25 to 100 g L^{-1}. The coating composition at different concentrations of aluminum oxide (wt.%) was given in Table 5. The coating composition is discussed later in Sect. 3.1.

2.3 Electroless plating process

Plating experiments were conducted by immersing the specimens in 200 mL plating solution for 1 h. Typically, a coating with a mass of at least 20 mg was predicted over this period. The effect of the following parameters on the electroless deposition rates was studied:

Table 3 The coating composition at different concentrations of sodium tungstate

Sodium tungstate concentration (g L^{-1})	Coating composition (wt.%)			
	Symbol	Nickel	Phosphorus	Tungsten
0	Base	90	10	0
5	W1	89.5	9	1.5
25	W2	89	6.5	4.5
45	W3	88.75	3.5	7.75
65	W4	87.25	2.75	10

Table 4 Composition of electroless plating bath used for Ni–P–Al_2O_3 coating

Chemicals	Concentration (g L^{-1})
Nickel sulfate, $NiSO_4 \cdot 6H_2O$	25
Aluminum oxide, Al_2O_3	25, 50, 75, 100
Sodium hypophosphite, $NaH_2PO_2 \cdot H_2O$	25
Sodium citrate, $Na_3C_6H_5O_7 \cdot 2H_2O$	50
Ammonium sulfate, $(NH_4)_2SO_4$	28
Lactic acid, $CH_3CHOHCOOH$	5×10^{-3}
Lead acetate, $Pb(CH_3CO_2)_2 \cdot 3H_2O$	2×10^{-3}

Table 5 The coating composition at different concentrations of aluminum oxide

Al_2O_3 concentration (g L^{-1})	Coating composition (wt.%)			
	Symbol	Nickel	Phosphorus	Aluminum oxide
0	Base	90	10	0
25	Al1	88.2	9.1	2.8
50	Al2	87.3	7.1	5.6
75	Al3	85.5	6.5	8
100	Al4	83.2	5.2	8.6

2.3.1 *Effect of temperature*

The deposition rate, calculated by weight gain (mg cm^{-2} h^{-1}), was measured as a function of the bath temperature in the range of 50–90 °C.

2.3.2 *Effect of pH*

It is usually impractical to use very low pH solutions because the deposition rates are low in such solutions [29, 30]. The deposition rate of alkaline electroless nickel baths relatively unaffected by bath pH within the normal range employed [31]. The baths are usually maintained at the proper pH by addition of ammonium hydroxide to replace evaporated ammonia and to neutralize acid produced by the deposition reaction.

In this work, the effect of pH on the deposition rate and phosphorus content was determined. The pH was studied in the range from 6 to 10.

2.3.3 *Effect of nickel sulfate concentration*

The deposition rate was measured as a function of the nickel sulfate concentration. The concentration was changed from 20 to 35 g L^{-1}.

2.3.4 *Effect of sodium hypophosphite (reducing agent)*

Sodium hypophosphite is one of the most common reducing agents used in the chemical reduction of nickel from aqueous solution. In this study, the deposition rate was measured as a function of sodium hypophosphite concentration. The concentration was changed from 15 to 30 g L^{-1}.

2.3.5 Effect of sodium citrate (complexing agent)

Generally, organic acids or their salts used in alkaline electroless nickel solutions for pH maintenance. In this study, the effect of sodium citrate concentration on the deposition rate was measured. The concentration was changed from 50 to 80 g L^{-1}.

2.3.6 Effect of deposition time

The deposition rate was measured as a function of time. The deposition time was changed from 20 to 90 min.

2.4 Testing methods

2.4.1 Coating chemical compositions

The coating composition was examined using the following procedures:

(1) The coating layer was stripped using 10% H_2SO_4 solution. The sample was then put as anode in an electroplating cell by which the coating layer was electrochemically dissolved in the solution, which was then diluted to 250 mL with bi-distilled water.
(2) The analysis was done using an Atomic Absorption Spectrophotometer (Perkin- Elmer 3100, Germany).
(3) The solution obtained was further diluted by dissolving 5 mL in bi-distilled water to 250 mL.

Nickel standard solutions for the elements to be detected were prepared as follows: 1 g of Ni metal was dissolved in (1 + 1) HNO_3 and diluted to 1 L with 1% (v/v) HNO_3. This standard solution can be used to detect Ni concentration till 7.0 ppm. Each detected element has its wavelength. For Ni, the wavelength is 232 nm in air–acetylene in flame gases.

The coatings were converted to atomic vapor in an air–acetylene flame. Such vapor can absorb light from the primary light source (Hollow cathode lamp). The light source emits a spectrum specific to the elements of which it is made, which is focused through the sample cell in the monochromator. The light source was electronically modulated to differentiate between the light from the source and emission from the sample cell. An electric current is produced depending on the light intensity and is electronically processed by the instrument. The instrument measures the amount of light attenuation in the sample cell and converts those readings to actual sample concentration.

2.4.2 Coating thicknesses

The coating thickness was measured by a coating thickness meter (Positector 6000, Model F1, Germany). The Positector is an accurate instrument based on adjusting the gage by taking the reading of a blank sample with no coating as zero and measuring the coated part. The difference between uncoated and coated values expresses the coating thickness.

The thickness of electroless nickel coating necessary to provide effective corrosion protection to steel depends on surface conditions; as little as 5 μm electroless nickel provides effective protection to polished steel whereas 50 μm or more may be necessary to protect a very rough surface. Generally, the thickness of all coatings used in this study ranged from 8 to 12 μm.

2.4.3 Hardness measurements

Vickers micro-hardness of the coating layer was measured under 50 g load using a Shimdsu Hardness tester. The diamond was pressed into the surface of the specimen material at a load of 50 g for 15 s. The diamond produced a square indentation and the average of the diagonal lengths was taken. The average of three readings was recorded.

2.4.4 Wear-resistance measurements

The wear-resistance was measured using cylindrical-shaped specimens of dimensions: 8-mm diameter and 12-mm height at a speed of 50 rpm for 30 min at 1.5 bars. The load range was 0.1–6 bars and the speed range was 0–1,000 rpm for up to 10 h.

2.4.5 Electrochemical impedance spectroscopy

The corrosion behavior was monitored using electrochemical impedance spectroscopy (EIS) during immersion in 3.5% NaCl solution open to air and at room temperature for up to 14 days.

A three-electrode set-up described elsewhere [32] was used with impedance spectra being recorded at the corrosion potential E_{Corr}. A saturated calomel electrode (SCE) was used as reference. It was coupled capacitatively to a Pt wire to reduce the phase shift at high frequencies. EIS was performed between 0.01 Hz and 65 kHz frequency range using a frequency response analyzer (Autolab PGSTAT 30, Eco-Chemie). The amplitude of the sinusoidal voltage signal was 10 mV.

2.4.6 Surface characterization

Energy-dispersive spectrometry. SEM images of the samples immersed in NaCl for 14 days, washed with deionized water and then dried were obtained using a digital scanning electron microscope (Model JEOL JSM 5410, Oxford Instruments, Japan). Microprobe analysis was performed using energy dispersive spectrometry, EDS (Model 6587, Pentafet Link, Oxford microanalysis group, UK).

X-ray diffraction. The solid corrosion products after 2 weeks in NaCl were characterized on the metallic surface, after drying the corroded specimen with methanol, by X-ray diffractometry (XRD). XRD analysis was performed using a Bruker machine, (Model D8, 40 kV, 40 mA, Cu Kα ADVANCE, Germany).

Surface morphology. Corrosion morphology was examined by metallurgical microscope, fitted with a digital camera.

3 Results and discussion

3.1 Effect of the experimental parameters

3.1.1 Effect of nickel ion concentration

Figure 1 shows the effect of the nickel concentration on deposition rate of electroless nickel deposition. The deposition rate increases as nickel ion concentration increases up to 25 g L^{-1}. At higher nickel ion concentration (up to 30 g L^{-1}), the deposition rate increases slightly and gives imperfect brightness as evidenced by visual inspection and optical microscope. Increasing the nickel ion concentration up to 35 g L^{-1} has no detrimental effect on the deposition rate. However, it adversely affects the brightness.

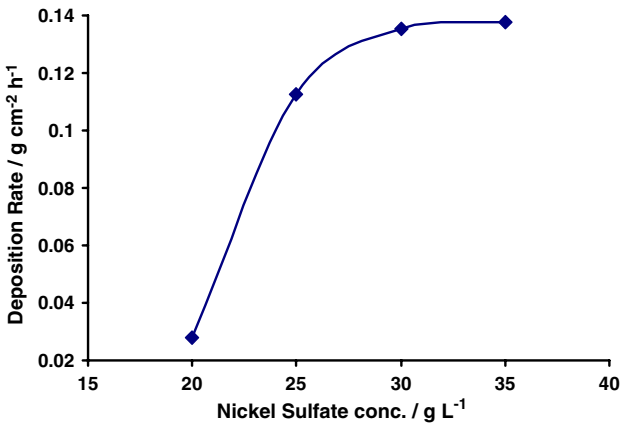

Fig. 1 Effect of nickel sulfate concentration on the deposition rate of electroless nickel. Bath composition: nickel sulfate 20–35 g L^{-1}, sodium hypophosphite 15 g L^{-1}, sodium citrate 50 g L^{-1}, ammonium sulfate 30 g L^{-1}, lead acetate 2 g L^{-1}, pH 9, temp. 90 °C, and time 60 min

3.1.2 Effect of sodium citrate concentration

Sodium citrate is used as a complex agent during nickel deposition. Figure 2 shows that the highest nickel deposition rate was obtained at 50 g L^{-1} sodium citrate concentration. Increasing the concentration of sodium citrate >50 g L^{-1} decreases the deposition rates. These results can be explained as follows:

- At low sodium citrate concentration (50 g L^{-1}), the bath is unstable and spontaneously decomposes; this is because, the citrate is a strong complexing agent used to prevent the precipitation of nickel hydroxide or basic nickel salts which have a negative effect on the deposition rate.
- The decrease in deposition rate at higher sodium citrate concentration (>50 g L^{-1}) is due to the decrease in concentration of free ions and the metal ions take on the characteristics of complex or chelated nickel ions.

3.1.3 Effect of sodium hypophosphite concentration

According to Fig. 3, the deposition rate of electroless nickel increases with increase in sodium hypophosphite concentration up to 25 g L^{-1}. Increasing the hypophosphite concentration >25 g L^{-1} decreases the deposition rate. Based on the results in Fig. 3, the following conditions should be considered:

(1) The concentration of hypophosphite should lie between 20 and 25 g L^{-1}.
(2) At higher concentration of hypophosphite (30 g L^{-1}) the stability of the plating bath is lowered, indicating that a stabilizer must be used.
(3) Increasing the $H_2PO_2^-$ concentration results in an increase in the phosphorus content of the deposit (Fig. 4).

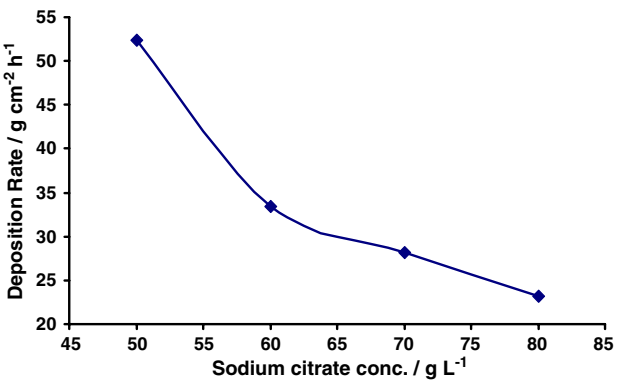

Fig. 2 Effect of sodium citrate concentration on the deposition rate of electroless nickel

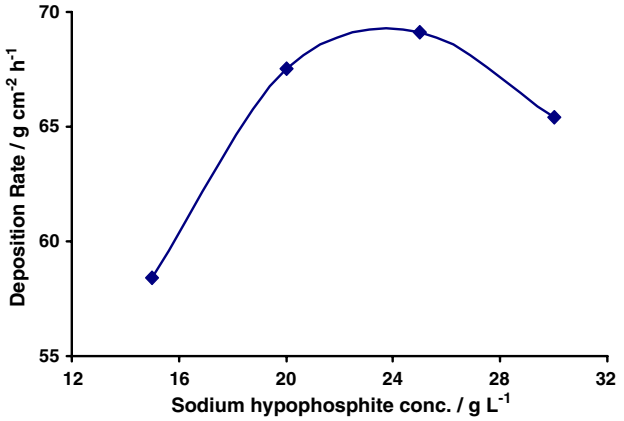

Fig. 3 Effect of sodium hypophosphite concentration on the deposition rate of electroless nickel

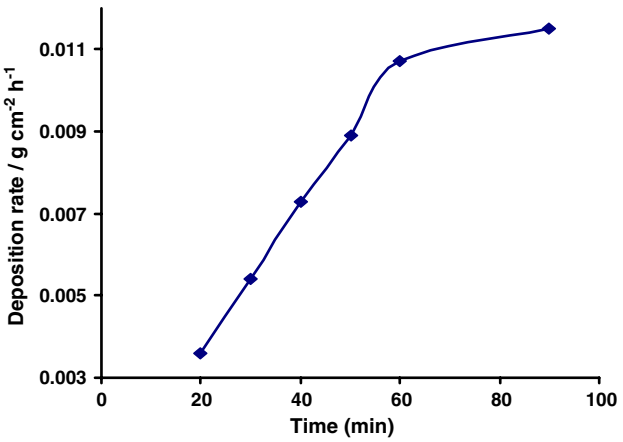

Fig. 5 Effect of deposition time on the deposition rate of electroless nickel

3.1.4 *Effect of the deposition time*

The deposition rate of electroless nickel increases linearly with time from 20 to 60 min (Fig. 5). Increasing the deposition time over 60 min was found to have no marked effect on the deposition rate. The deposition rate is almost constant in the range 60–90 min. Moreover, increasing the time of deposition is economically unattractive for industrial applications.

3.1.5 *Effect of bath temperature*

Generally, the deposition rate of electroless nickel increases sharply when the temperature rises from 50 to 90 °C (Fig. 6). However, the deposition rate is almost constant in the range 70–80 °C. Raising the temperature from 80 to 90 °C increases the deposition rate. However, at high temperature, the coating appears dull. Therefore, the best temperature for good electroless nickel is 70 °C.

According to Fig. 6, noticeable deposition rates are achieved at slightly lower temperature (60 °C). This result confirms the suitability of this type of bath for metallizing non-conductors with poor temperature resistance, e.g., ABS, polymers.

3.1.6 *Effect of solution pH*

Changing the pH from 6 to 7 has no noticeable effect on the deposition rate (Fig. 7). The deposition rates increased sharply with increasing pH from 6 to 10. Increasing the pH (from 9 to 10) decreases the deposition rates. At pH 10, the solution turns turbid due to precipitation of basic nickel salt or complex.

The pH can be maintained within its operating range by adding ammonium hydroxide to maintain the intense blue

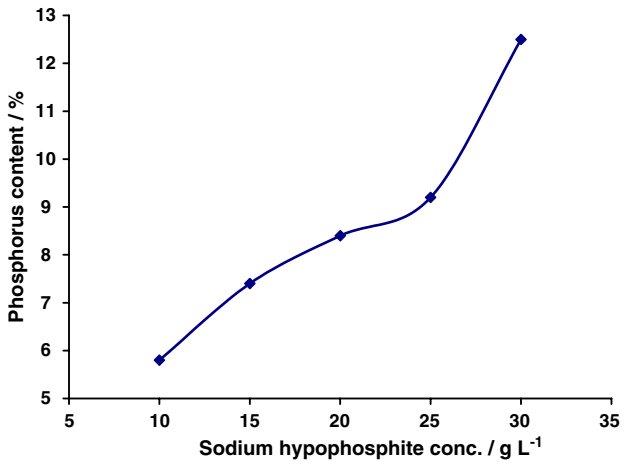

Fig. 4 Effect of sodium hypophosphite concentration on the phosphorous content

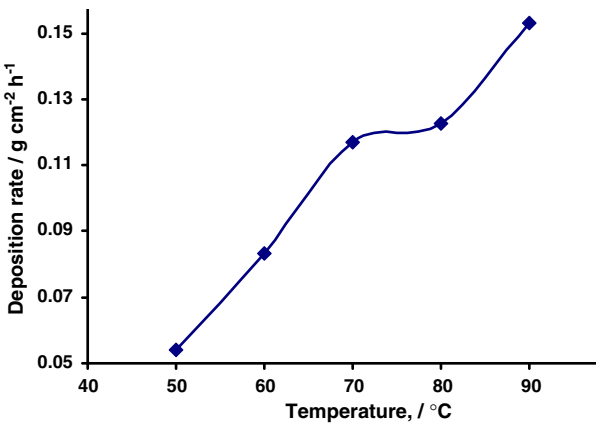

Fig. 6 Effect of temperature on the deposition rate of electroless nickel

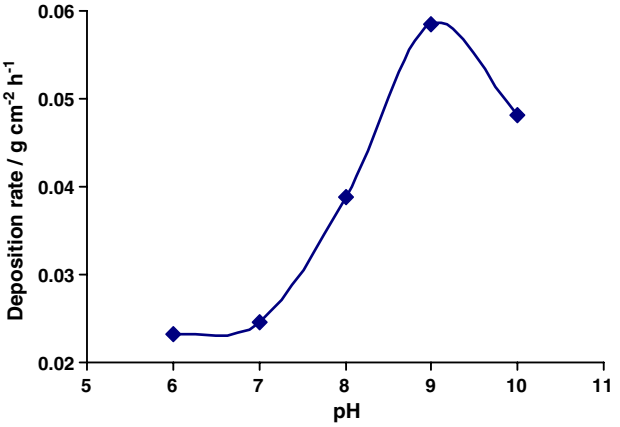

Fig. 7 Effect of pH on the deposition rate of electroless nickel

color of the nickel ammine complex. When the pH decreases, the color of the solution changes from dark blue to blue-green, to green, at which ammonium hydroxide must be added to restore the pH.

The solution pH has a deleterious effect on the coating composition especially on the phosphorus deposition as shown in Fig. 7. The phosphorus content decreases sharply with increasing pH in the alkaline range (>9).

3.1.7 Effect of lead acetate concentration

Lead acetate is used as an inhibitor for nickel reduction. The change in deposition rate as a function of lead acetate concentration is shown in Fig. 8. The nickel deposition rate is dramatically decreased especially between 2 and 5 mg L^{-1} lead acetate. At 5 mg L^{-1} the nickel deposition rate flattens out and approaches zero. In order to achieve a good deposition rate, the lead acetate concentration should not be less than 2 mg L^{-1}.

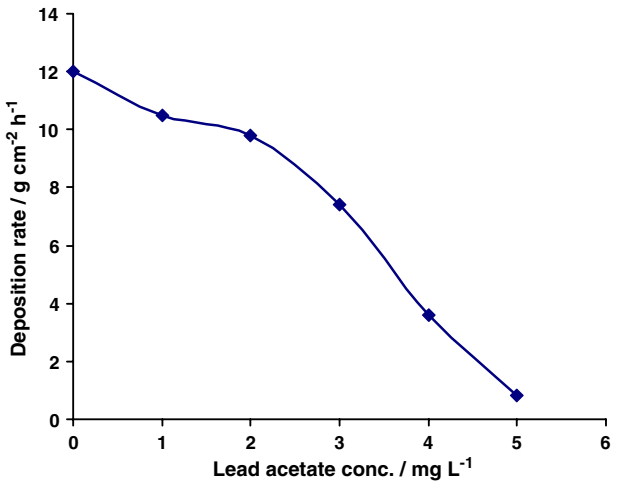

Fig. 8 Effect of lead acetate concentration on the deposition rate (mg/cm/h) of electroless nickel

This rules out the assumption that inhibition of nickel deposition is realized through complex formation between lead acetate inhibitor and the nickel ion, which leads to reduction of the free nickel ion concentration and thus inhibits the reduction of nickel.

3.2 Coating performance

3.2.1 Micro-hardness

Electroless Ni–P coatings are considerably harder and more wear-resistant than conventional electroplated nickel and have, therefore, found many industrial applications. Results showed that Ni–P coatings have a Vickers hardness of about 570 kg mm^{-2} which is in agreement with literature data ranging from 500 to 600 kg mm^{-2} [33]. The hardness can be even further increased (to about 1,000 kg mm^{-2}) by heat treatment for 1 h at 400 °C [33]. However, surface micro-cracks can be observed after heat treatment. It seems that heat treatment results in increased hardness by a precipitation-hardening mechanism.

The variation in micro-hardness of Ni–P–Al_2O_3 composite coatings versus the Al_2O_3 concentration in the electroless nickel bath is shown in Fig. 9. The micro-hardness, generally, increases with increasing incorporation of Al_2O_3 ratio in the deposit up to 75 g L^{-1}. The highest micro-hardness was obtained from the sample that contains 75 gm L^{-1} alumina (sample Al3). Further increase in the alumina concentration has no marked effect on the micro-hardness.

Micro-hardness of the as-plated coatings was plotted as a function of the sodium tungstate concentration in the plating bath, as shown in Fig. 10. Increasing the tungstate concentration increases the micro-hardness of electroless Ni–W–P. Ni–W–P coatings showed much higher hardness compared with Ni–P and Ni–P–Al_2O_3 coatings. It can be seen from Fig. 10 that there is a significant increase in the

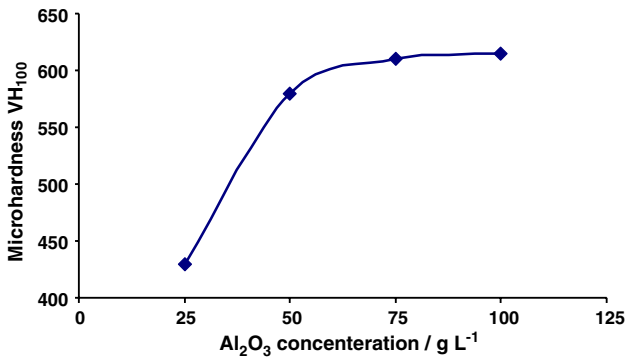

Fig. 9 Effect of the alumina ratios on the micro-hardness of Ni–P–Al_2O_3

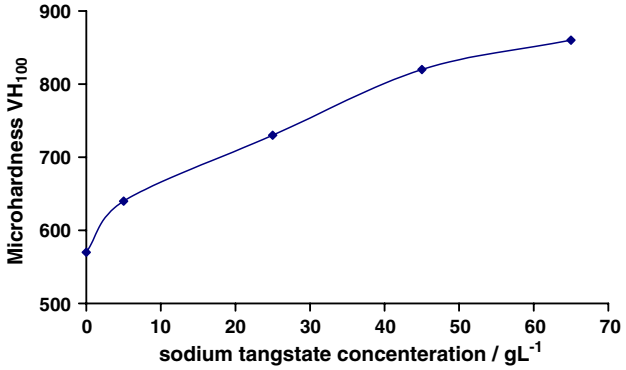

Fig. 10 Effect of the tungstate ratios on the micro-hardness of Ni–P–W

micro-hardness for all Ni–W–P deposits in comparison to Ni–P deposit, although they have less phosphorus contents.

3.2.2 *Wear-resistance*

Generally, the wear-resistance of electroless nickel coatings containing 10% phosphorus improves with addition of tungsten or alumina (Figs. 11, 12). The weight loss due to wear decreases with increasing alumina ratio in the coatings (Fig. 11). The highest wear-resistance was obtained from samples Al3 and Al4, which contain 75 and 100 g L^{-1} alumina respectively.

The addition of tungstate sharply improves the wear-resistances; this can be attributed to formation of a tungstate phosphide outer layer. The highest wear-resistance was obtained from the lowest tungstate ratios. Increasing the tungstate concentration more than 5 g L^{-1} improves the wear-resistance, but the coating performance is less than that obtained from the coating containing 5 g L^{-1} tungsten. According to Figs. 11 and 12, tungstate coatings have much higher wear-resistance compared with Ni–P and Ni–P–alumina coatings.

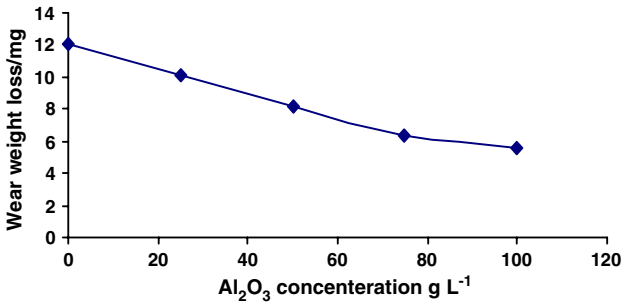

Fig. 11 Effect of the alumina ratios on the wear-resistance of Ni–P–Al_2O_3

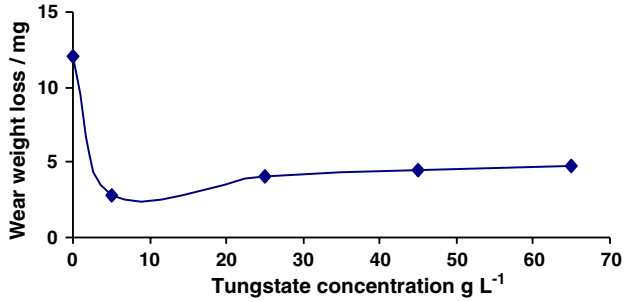

Fig. 12 Effect of the tungstate ratios on the wear-resistance of Ni–P–W

3.2.3 *Corrosion resistance*

Electrochemical impedance spectroscopy (Fig. 13) showed that Ni–P coatings showed a distinct improvement in corrosion resistance compared with as-polished ones. The surface resistance of the as polished samples was $0.07 \times 10^4\ \Omega\ cm^2$. The surface resistance of Ni–P was about 10 times greater ($0.78 \times 10^4\ \Omega\ cm^2$) than the as-polished specimens. Improving the corrosion resistance was attributed to formation of a protective layer of metallic nickel and nickel phosphide that act as a barrier to oxygen diffusion to the metal surface [34–37]. However, pitting corrosion and micro-cracks were observed after 2 weeks of immersion in NaCl solution (Fig. 14).

The presence of alumina improves the corrosion resistance of steel in NaCl (Fig. 13). The surface resistance rose sharply to $7.00 \times 10^4\ \Omega\ cm^2$ which is 100 times higher than that obtained from the as-polished samples. Detailed corrosion studies from previous work [35–37] confirmed the formation of metallic nickel and nickel phosphide layer due to presence of alumina over steel substrate. However, the layer was too thick and hence severe micro-cracks as well as pitting corrosion were observed at the surface after 2 weeks of immersion in 3.5% NaCl solution (Fig. 15).

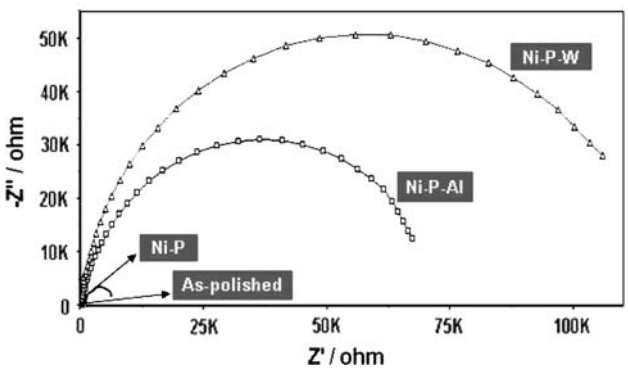

Fig. 13 Electrochemical impedance spectra after 2 weeks of immersion in 3.5% NaCl solution

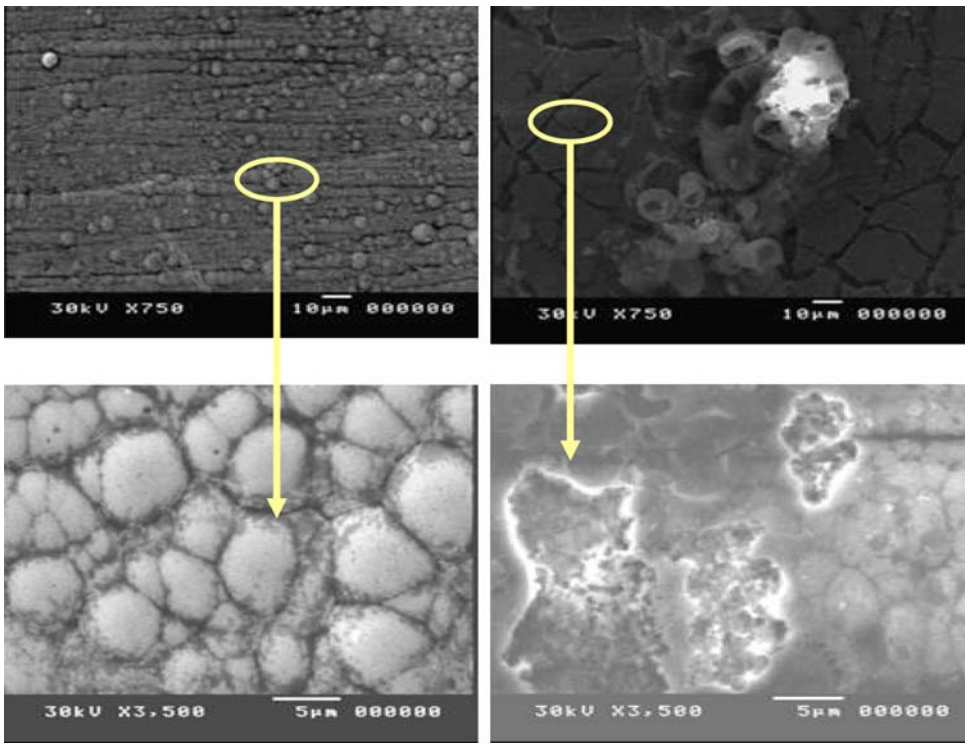

Fig. 14 SEM of Ni–P before (left) and after (right) corrosion

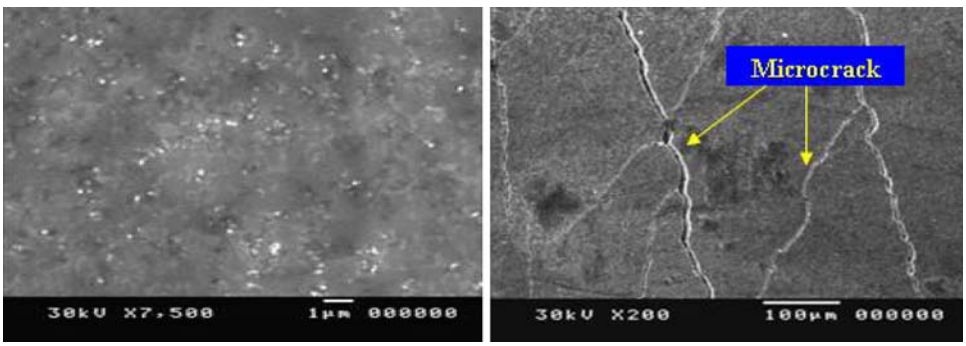

Fig. 15 SEM of Ni–P–alumina before (left) and after (right) corrosion

The corrosion resistance of steel improved sharply due to tungstate coatings According to the EIS measurements (Fig. 13), increasing the tungsten ratio to 5 g L^{-1} improves the surface resistance to 1.20×10^4 Ω cm^2 which is 180 times that of as-polished samples. Tiny pits were observed after 2 weeks immersion in NaCl solution (Fig. 16). It was suggested that tungstate coatings have a dual effect. The first is to enhance the surface resistance by forming corrosion resistant films of tungsten phosphide. The second is the "buffer' action of this film to reject chloride ions from

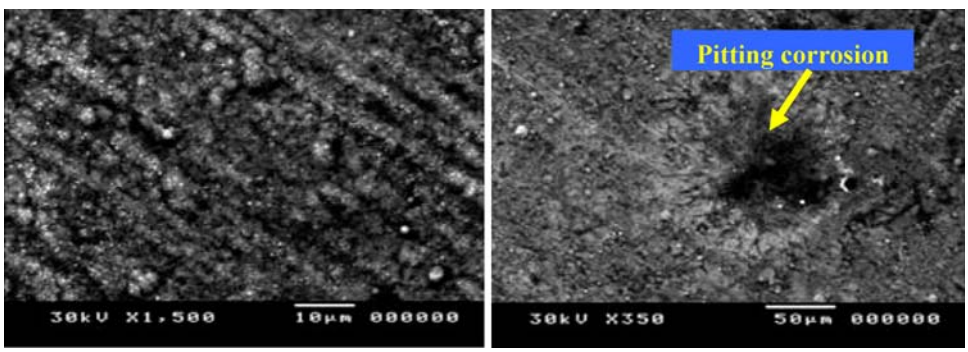

Fig. 16 SEM of Ni–P–W before (left) and after (right) corrosion

the metal surface as confirmed by EDS analysis and hence improve the pitting corrosion resistance [35–37].

4 Conclusions

The effect of experimental parameters such as temperature, pH, deposition time, and the chemical composition of the bath on the electroless deposition of Ni–P alloy coatings onto steel substrates was studied. The coating performance increased with the addition of W and alumina. However, the best micro-hardness, wear-resistance, and corrosion protection performance was obtained from tungsten containing coatings. The corrosion resistance was sharply improved due to the formation of a highly protective tungsten phosphide phase.

References

1. Mallory GO, Hajdu JB (1990) In: Electroless plating: fundamentals and applications, American Electroplaters and Surface Finishers Society, Orlando, FL, p 1, Chapter 4
2. Sue JA, Chang TP (1995) J Surf Coat Technol 76–77:61
3. Chiba Y, Ornura T, Ichimura H (1993) J Mater Res 8:1109
4. Safranek WH (1986) The properties of electrodeposited metals and alloys, 2nd edn. American Electroplaters and Surface Finishers Society, Orlando, FL, p 345
5. Gawrilov G (1979) Chemical electroless nickel plating. Portculli Press, Surrey, UK
6. Riedel W (1991) W-electroless plating. ASM International, Ohio
7. Di Bari GA (2003) Basic information on finishing processes. Plat Surf Finish No. 8
8. Macko R, Mason T (2000) Plat Surf Finish 3:140
9. Baudrand D (1999) Plat Surf Finish 11:44
10. Tung S and Devin T (2002) the 22nd Electrochemical Society Meeting, Meeting Abstracts, Salt Lake City, Utah, G1–25
11. Yan H (2001) New techniques in electroless nickel and composite plating. Industry of National Defense Press, Beijing, p 1
12. Stevanovic R, Stevanovic J, Despic A (2002) J Appl Electrochem 31:855–862
13. Wang C, Cai W-B, Wang W-J, Liu H-T, Yu Z-Z (2003) Surf Coat Technol 158:300
14. Wang Y, Xio C, Ding Z (1992) Plat Surf Finish 3:57
15. Amyanov S, Steenhaut O, Krasteva N et al (1996) J Electrochem Soc 143:3692
16. Nash P (1991) Phase diagrams of binary nickel alloys. ASM International, June, p 235
17. Zhang BW, Hu WY, Zhang QL, Qu XY (1996) Mater Charact 37:119
18. Ytsai Y, Wu FB, Chen Y et al (2001) Surf Coat Technol 146–147
19. Boanani M, Cherkaoui F, Fratesi R et al (1999) J Appl Electrochem 29:637
20. Zhao Q, Liu Y, Muller-Steinhagen H et al (2002) Surf Coat Technol 155:279
21. Liu Y, Zhao Q (2003) Trans IMF 81(5):1
22. Lee CY, Lin KL (1994) Jpn Appl Phys 33(8):4708
23. Hur KH, Jeong JH, Lee DN (1991) J Mater Sci 26(8):2037
24. Gopal IR (1992) Bull Electrochem 8:384
25. Dennis JK, Such TE (1986) Nickel and chromium plating, 2nd edn. Butterworth and Co. Ltd.
26. Oberle R, Scanlon MR, Cammarata RC et al (1995) Appl Phys Lett 66:19
27. Mueller B, Ferkel H (1998) Nanostruct Mater 10:1285
28. Jakob C, Erler F, Nutsch R et al (2000) Proceedings: 97th meeting of the electrochemical society, Toronto, vol 2000–1, 329
29. Talmey P and Gutzeit G (1956) US Patent 2762723
30. Gorbunova KM, Nikiforova A (1954) J Phys Chem USSR 28883
31. Alberts GS, Wright RH, Parker C (1966) J Electrochem Soc 113:687
32. Hamdy AS, Beccaria AM, Spiniello R (2001) Corros Prev Control 48:101
33. Gutzeit E, Mapp ET (1965), Corros Technol 3:331
34. Hamdy AS, Hady H, Shoeib MA et al (2007) Advanced electroless Ni–P coatings containing tungsten or nano-sized alumina particles: The effect of the experimental parameters. Presented at the European Corrosion Congress, EurroCorr -Germany
35. Hamdy AS, Hady H, Shoeib MA et al (2007) Electrochemical impedance studies on Ni–P–W and Ni–P–Al_2O_3 nano-composite alloy coatings in 3.5% NaCl. Presented at the European Corrosion Congress, EurroCorr-Germany
36. Hamdy AS, Hady H, Shoeib MA et al (2007) Newly developed corrosion resistant nano-composite alloy coatings for steels. Presented at the "Corrosion and Coatings Challenges in Industry" Symposium, 88th Annual Meeting, Boise State University, Boise, ID, June 19, co-located with the 62nd Annual Meeting of the American Chemical Society
37. Hamdy AS, Hady H, Shoeib MA et al (2007) Surf Coat Technol 202:162–171